

Available online at www.sciencedirect.com

ScienceDirect

journal homepage: www.e-jds.com

Original Article

Advancing osseointegration research: A dynamic three-dimensional (3D) *in vitro* culture model for dental implants

Keiji Komatsu ^{a*†}, Denny Chao ^{b†}, Takanori Matsuura ^a,
Daisuke Kido ^a, Takahiro Ogawa ^{a,b}

^a Weintraub Center for Reconstructive Biotechnology, UCLA School of Dentistry, Los Angeles, CA, USA

^b Division of Regenerative and Reconstructive Sciences, UCLA School of Dentistry, Los Angeles, CA, USA

Received 4 June 2024; Final revision received 22 June 2024

Available online 3 July 2024

KEYWORDS

Hydrophilic materials;
Osseointegration;
Osteoblasts;
Surface properties

Abstract *Background/purpose:* *In-vitro* studies are essential for understanding cellular responses, but traditional culture systems often neglect the three-dimensional (3D) structure of real implants, leading to limitations in cellular recruitment and behavior largely governed by gravity. The objective of this study was to pioneer a novel 3D dynamic osteoblastic culture system for assessing the biological capabilities of dental implants in a more clinically and physiologically relevant manner.

Materials and methods: Rat bone marrow-derived osteoblasts were cultured in a 24-well dish with a vertically positioned dental implant. Controlled rotation using a 3D rotator with 3° tilts was applied. Cell attachment, proliferation, and differentiation on implant surfaces were evaluated in response to different surface topographies, physicochemical properties, and local environments.

Results: Among the tested rotational speeds (0, 10, 30, 50 rpm), optimal osteoblast attachment and proliferation were observed at 30 rpm. A linear correlation was found between cell attachment and rotation speed up to 30 rpm, declining at 50 rpm. Alkaline phosphatase (ALP) activity and mineralized matrix formation were elevated on newly acid-etched, hydrophilic surfaces compared to their 4-week-old hydrophobic surfaces. Sandblasted implants showed higher ALP activity and matrix mineralization. Adding N-acetyl cysteine to the culture medium increased ALP activity and mineralization.

Conclusion: Osteoblasts successfully attached, proliferated, and mineralized on dental implants *in vitro* under optimized dynamic conditions. This system differentiated the biological capabilities of implants with varying surface topographies, wettability, and biochemically modulated environments. These findings support developing a 3D dynamic dental implant

* Corresponding author. Weintraub Center for Reconstructive Biotechnology, UCLA School of Dentistry, 10833 Le Conte Avenue B3-087, Los Angeles, CA 90095, USA.

E-mail address: kkomatsu@ucla.edu (K. Komatsu).

† These two authors contributed equally to this work.

culture model, advancing osseointegration research and innovating dental implant designs.
 © 2025 Association for Dental Sciences of the Republic of China. Publishing services by Elsevier B.V. This is an open access article under the CC BY-NC-ND license (<http://creativecommons.org/licenses/by-nc-nd/4.0/>).

Introduction

Osseointegration is a dynamic process governed by intricate interactions between biological molecules and cells with implant surfaces and has been a cornerstone in implant research and titanium science.^{1,2} A focal point in this domain has been the enhancement of osseointegration through improvements in implant surface properties.^{3,4} Microrough titanium surfaces, prevalent in contemporary dental implants, have demonstrated superior bio-capability compared to smooth, machined predecessors.⁵ These surfaces not only augment cell and bone retention through enhanced mechanical interlocking^{6–8} but also foster the functionality of osteogenic cells.^{9–11} Specifically, mesenchymal stem cells adhering to microrough surfaces is able to sense the surface texture and promote their differentiation,^{12–14} thereby expediting osseointegration.^{15,16} Additionally, microrough surfaces contribute to the enhancement of mineralized tissue quality and interfacial bonding.^{17–19}

In vitro osteoblast culture has been essential in the development of such surface topographies, typically conducted on titanium disks within polystyrene dishes.^{20–22} The advantages of *in vitro* cell culture over *in vivo* animal experiments are diverse, including the ability to dissect osteoblast function event-by-event, test various types and stages of osteogenic cells, examine a plethora of biological markers relevant to osseointegration, conduct high-throughput screening, control culture conditions, and reduce costs and study time.^{23–25} In particular, rat-derived osteoblasts have higher reproducibility and greater mineralization efficiency than human-derived cells,²⁶ making them widely applicable in previous studies on titanium implants.^{12,13} This approach has proven essential for generating robust *in vitro* data that can refine hypotheses and experimental designs, facilitating the progression to more complex bioengineering studies.

However, disparities between results from *in vitro* and *in vivo* experiments underscore the pressing need for refinement in *in vitro* setups to better mimic real-life procedures and environments in implant dentistry.^{24,25,27} Titanium disks offer only a two-dimensional, flat, horizontal surface for cell adhesion, with cells predominantly adhering to these surfaces following gravity, regardless of surface properties, thereby diluting the effects of varied surface properties. This limitation is compounded by the failure of titanium disks to replicate the macroscopic form of dental implants, which include screw threads, inclines, valleys, peaks, and extensive undercuts along the gravity. Cell adhesion and subsequent expression of functional phenotypes should be extremely challenging for osteoblasts on dental implants compared to flat titanium disks. Moreover, fluid dynamics are significantly influenced by the

micro- and macroscopic forms of dental implants, regulating the speed and distribution of proteins and cells around implants,^{28–31} which is not considered in the current 2D cell cultures. Thus, the inherent limitation of static cultures on flat titanium specimens is evident.^{24,25,27}

The objective of this study is to pioneer a novel 3D dynamic osteoblastic culture system aimed at assessing the biological capabilities of dental implants in a more clinically and physiologically relevant manner. We hypothesize that osteoblasts can be cultured on dental implants reflecting real-life complexities, such as non-flat morphologies, without horizontal surfaces, by optimizing peri-implant fluid dynamics. To validate the reliability and usefulness of this system, we investigated its responsiveness to established osteoblast behavior on titanium and its sensitivity in discriminating between different surface topographies, wettability states of implants, and diverse osteogenic environments.

Materials and methods

Study design

We initially tested three different rotational speeds to identify the optimal rotation for the dynamic 3D culture system (Fig. 1A). Subsequently, the sensitivity of the culture system was evaluated based on osteoblast response to three key biological factors of implant research: 1) topography; 2) wettability; and 3) biochemically modulated local environments (Fig. 1B). This comprehensive approach designed to validate the capabilities of a 3D culture system for cell culture on dental implant surfaces.

Sample preparation

To investigate the sensitivity of the new culture method to implant surface characteristics, we prepared two types of implants with different surface topographies. First, we used commercially available sandblasted tapered implants (3.8 × 10.5 mm, BioHorizons, Birmingham, AL, USA) for the sandblasted implant group. Second, we created the acid-etched implant group by further acid-etching these sandblasted implants with 66% sulfuric acid at 120 °C for 90 s. Additionally, to test the impact of surface wettability, we prepared two sets of acid-etched implants: “new” implants, which were used immediately after acid etching, and “aged” implants, which were stored in the dark for four weeks post-etching. This approach is based on the phenomenon of the biological aging of titanium,³² where new implants are hydrophilic and aged implants become hydrophobic.

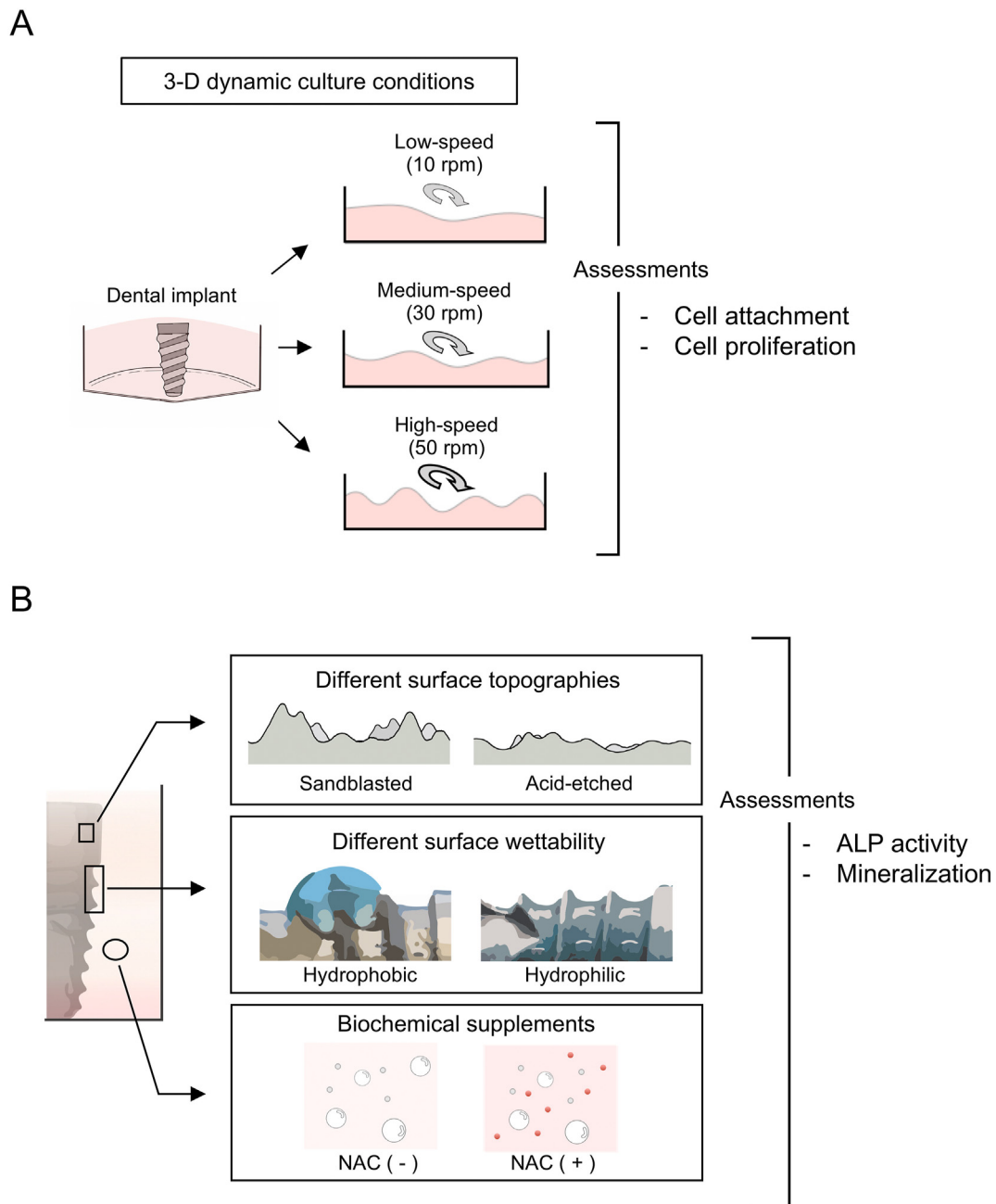


Figure 1 Study design. (A) Schematic illustration of the experimental setup designed to determine the optimal rotation speed for enhancing osteoblast attachment and proliferation on dental implant surfaces vertically positioned at the center of the well. (B) Overview of the experimental strategy to assess the sensitivity of the three-dimensional (3D) dynamic culture system. The sensitivity of the 3D culture system to discern three key factors—1) surface morphology, 2) wettability, and 3) biochemical supplements—was evaluated by examining osteoblast differentiation.

Surface characterization

Scanning electron microscopy (SEM; FEI, Hillsboro, OR, USA) was used to confirm the differences in surface morphology between sandblasted implants and acid-etched implants. Surface roughness parameters Ra and Rz were examined using a three-dimensional confocal scanning laser microscope (Keyence, Osaka, Japan). The surface wettability of implants was assessed by measuring the contact angle of a 3 μ L ddH₂O droplet.

Osteoblast cell culture

Bone marrow-derived osteoblastic cells were isolated from the femurs of 8-week-old male Sprague–Dawley rats, following established protocols.³³ Isolated cells were cultured in alpha-modified Eagle's medium with 15% fetal bovine serum, 50 μ g/mL ascorbic acid, 10 mM Na- β -glycerophosphate, 10⁻⁸ M dexamethasone, and antibiotics at 37 °C in 95% air and 5% CO₂. At 80% confluency, cells were detached using 0.25% trypsin–EDTA. For the setup of

dynamic culture conditions, implants were vertically placed in 14 mm-diameter wells of a 24-well culture dish and immobilized with 0.002 g adhesive cement (Sun Medical Co. Ltd., Shiga, Japan) (Fig. 2A). Then, 8×10^4 cells were seeded into each well (Fig. 2B). Immediately after cell seeding, the culture plates were subjected to dynamic conditions using a speed-controllable 3D rotator (PS-3D, Grant Instruments, Cambridge, UK) (Fig. 2C). The system tested three different rotational speeds—low (10 rpm), medium (30 rpm), and high (50 rpm)—to assess osteoblast response. Plates without rotational movement served as the static culture condition. Specifically, for testing the sensitivity of the dynamic culture to local biochemical environments, N-acetylcysteine (NAC) was added at a concentration of 1 mM to the culture wells concurrently with cell seeding, following previously established protocols.³⁴ The experiments were approved by the UCLA Animal Research Committee (ARC #2005-175-41E).

Quantification of attached and proliferated cells

The number of osteoblasts on implant surfaces at days 2, 4, and 6 was evaluated using a tetrazolium salt-based colorimetric assay (WST-1; Roche Applied Science, Mannheim, Germany), following established protocols.^{35,36} Cultured implants were treated with WST-1 reagent, and formazan

product was measured at 450 nm using a plate reader (BioTek Instruments, Winooski, VT, USA). Additionally, to visualize cell distribution, cells were fixed in 10% formalin and stained with Rhodamine-phalloidin (actin filaments, red) and DAPI (nuclei, blue).

Alkaline phosphatase (ALP) activity

To monitor early cell differentiation, ALP activity on cultured implants was evaluated on day 5. ALP is an early biomarker of osteoblast differentiation and typically changes early days of culture in rat-derived osteoblasts, reflecting the characteristics of titanium surfaces.¹³ Implants were treated with 250 μ L p-nitrophenylphosphate (Wako Pure Chemicals, Richmond, VA, USA), and incubated at 37 °C for 15 min. ALP activity, indicated by the amount of nitrophenol released, was measured at 405 nm using a plate reader.

Alizarin red staining and quantitative analysis

Mineralized matrix formation is a late-stage marker of osteoblast differentiation, occurring after the rise in ALP activity. Based on previous studies, we evaluated mineral deposition on the implant surface using alizarin red staining

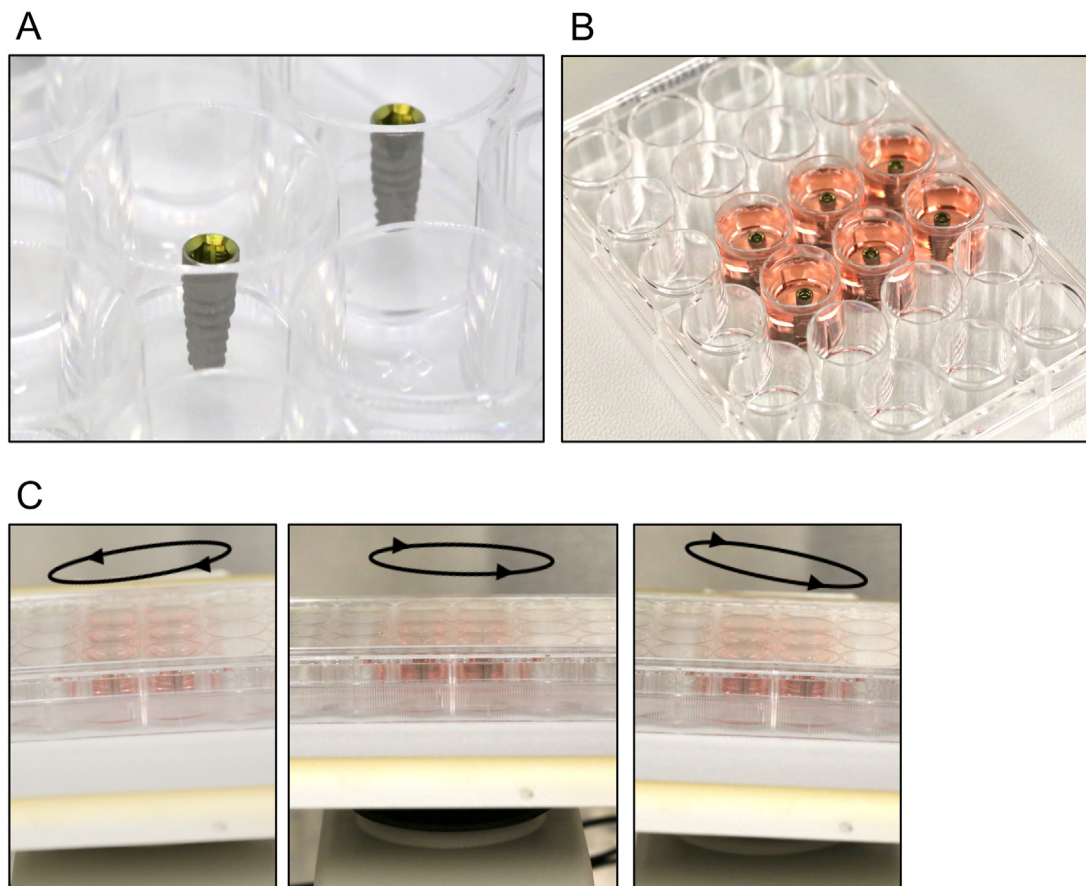


Figure 2 A dynamic three-dimensional culture model for dental implants. (A) A dental implant standing upright was secured using 0.002 g of resin bonding cement in a well of a 24-well cell culture-grade polystyrene dish. (B) Dental implants were fully immersed in the culture medium. (C) The culture dish underwent continuous rotational motion with 3° tilts and variable speed.

on day 10.^{37,38} Implants were fixed in 10% formalin, and stained with 1% alizarin red solution (Sigma–Aldrich, St. Louis, MO, USA) for 5 min. The stained implants were dissolved in 10% acetic acid for 30 min, then 10% ammonium hydroxide was added. The optical density was measured at 405 nm using a microplate reader.

Statistical analysis

All cell culture experiments were performed in triplicate. Results are presented as means \pm standard deviation (SD). Statistical analyses were conducted using GraphPad Prism 9.0 software (GraphPad Software, La Jolla, CA, USA). One-way ANOVA with Bonferroni post hoc tests compared cell attachment and proliferation among different rotational speeds. Unpaired t-tests determined differences between two groups. A *P*-value <0.05 was considered significant.

Results

Implant surface topography

SEM analysis of sandblasted and acid-etched implants revealed distinct characteristics. Sandblasted implants exhibited supra-micron scale, coarse roughness with randomly distributed craters resulting from blasting particles, while acid-etched implants displayed a finer, micro-scale, homogeneous roughness (Fig. 3A). The average surface roughness (*R*_a) was approximately four times higher for sandblasted surfaces (Fig. 3B), with a corresponding increase in the maximum height difference (*R*_z). Cross-sectional profiling confirmed significantly greater fluctuation in sandblasted surfaces compared to acid-etched surfaces, consistent with quantitative roughness values.

Wettability of new and aged implants

Titanium implants undergo biological aging, losing hydrophilicity over time. To replicate this phenomenon, acid-etched surfaces were created at different aging stages: immediately after acid-etching and four weeks post-etching. Droplet assays demonstrated rapid spreading on new implants, indicating hydrophilicity, while aged implants exhibited spherical droplets, indicative of hydrophobicity. Contact angle measurements confirmed this observation, with aged implants exhibiting a contact angle of $124.5 \pm 8.8^\circ$ compared to 0° for freshly acid-etched implants (Fig. 3C). Thus, implants with identical topographies manifested distinct wettability properties.

Rotation speed optimization for osteoblastic dynamic culture

We hypothesized that there would be insufficient osteoblast attachment to vertically standing dental implants under static conditions. To address this limitation, we explored dynamic culture conditions using a speed-controllable, 3D rotator to enhance osteoblast attachment. The rotator was capable to maintain the rotational movement while tilting the culture dish, as shown in Fig. 2.

Cell attachment was maximized at 30 rpm, doubling the number of cells compared to static culture (Fig. 4A). Fluorescent microscopic observation confirmed increased cell attachment with dynamic cultures, peaking at 30 rpm and evenly distributed across implant zones. However, cell colonization was sparse in static cultures (0 rpm) and dynamic cultures at 50 rpm, particularly in the mid zone (Fig. 4B).

Cell proliferation in dynamic cultures with varying rotation speed

We further validated the sensitivity of osteoblast behavior to rotation speed in dynamic cultures. Given the potential for cell detachment due to fluid dynamics in later stages of culture, it was imperative to assess cell proliferation over time.

Dynamic cultures with varying rotation speeds consistently exhibited rotation speed-sensitive osteoblast behavior. Cell proliferation assays revealed the highest cell counts on implants cultured at 30 rpm after 4 and 6 days, while dynamic cultures at 50 rpm were ineffective and even resulted in decreased cell numbers on day 6 compared to static culture (Fig. 5). Regression analysis demonstrated a quadratic relationship between cell number and rotation speed, peaking at 30 rpm ($R^2 = 0.881$). Exclusion of 50 rpm from the analysis revealed a linear correlation ($R^2 = 0.995$), indicating increased osteoblast attachment with higher rotation speeds (Fig. 6).

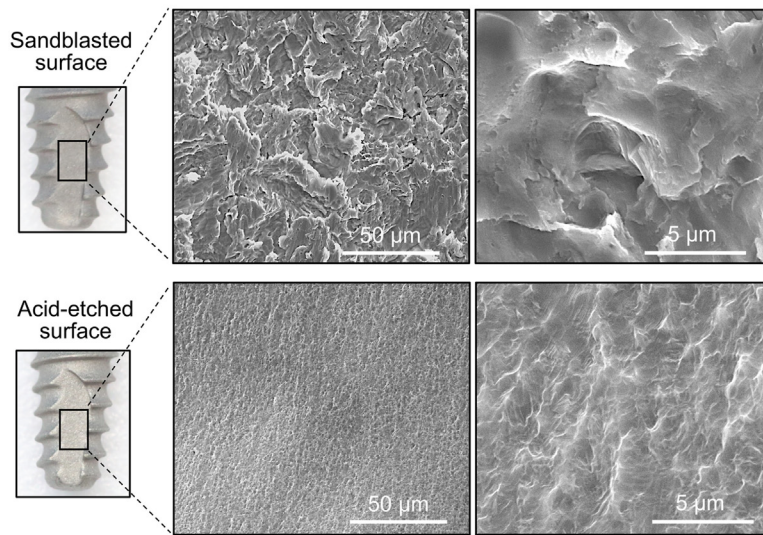
These findings from continuous cell counts over days 2, 4, and 6, along with regression analyses, collectively underscored the significant enhancement in osteoblast attachment and function on standing dental implants in dynamic cultures compared to the static culture. However, optimal rotation speed is crucial to maximize cell attachment and function, as excessive rotation speed can compromise cell behavior even more than static culture.

Osteogenic response to diverse surface properties and local environments

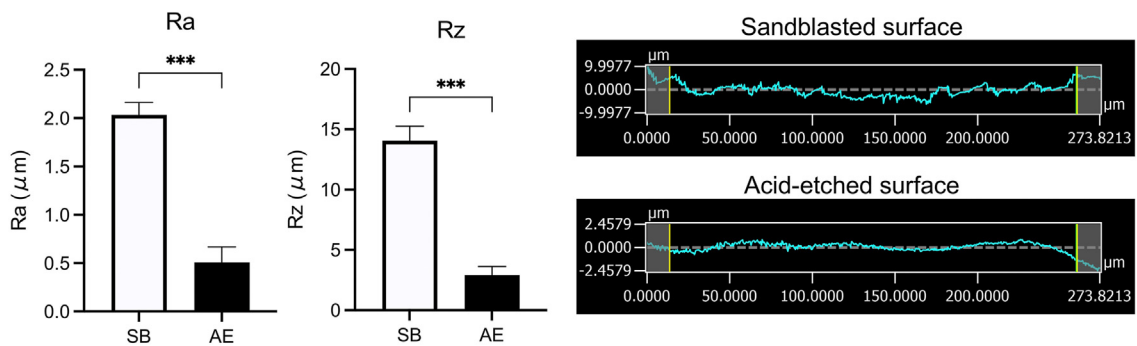
Next, we investigated whether the attached osteoblasts successfully followed the anticipated course of differentiation/maturation, ultimately leading to mineralization. Various influencing factors on osteoblastic differentiation, such as different surface topographies, levels of wettability, and local environments, were examined. These experiments utilized optimized dynamic cultures with a rotation speed of 30 rpm.

Osteoblasts on sandblasted surfaces exhibited higher ALP activity at day 5 and increased matrix mineralization at day 10 compared to acid-etched surfaces (Fig. 7A and B). Additionally, hydrophilic acid-etched surfaces showed higher ALP activity and mineralization than hydrophobic counterparts (Fig. 7C and D). Furthermore, dynamic cultures with NAC supplementation promoted robust ALP activity and mineralization (Fig. 7E and F). These findings underscore the sensitivity of the optimized dynamic culture system in discerning osteoconductive potential arising from different surface properties and local environments.

A



B



C

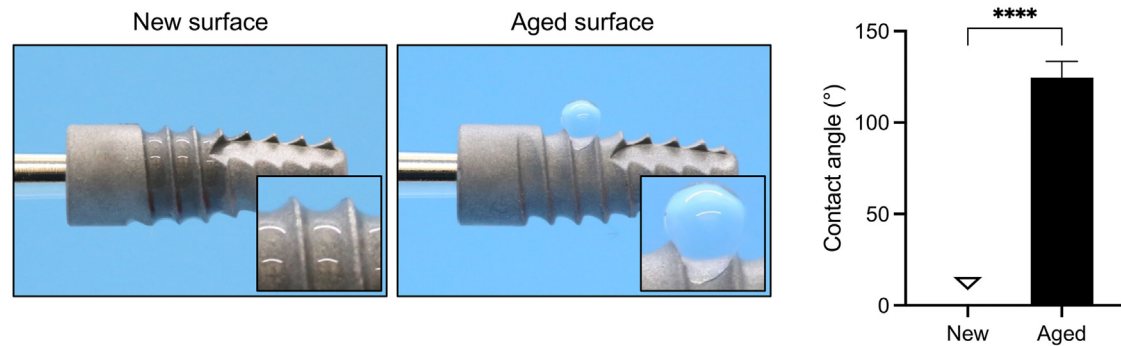


Figure 3 Surface characterization of dental implants. (A) Scanning electron microscopy (SEM) images of sandblasted and acid-etched implants are shown, including both low- and high-magnification views. (B) Quantitative assessment of surface roughness. An average roughness (Ra) and peak-to-valley roughness (Rz) parameters of sandblasted and acid-etched implant surfaces, along with representative images of roughness profiles. (C) Creation of hydrophilic and hydrophobic implants with identical surface morphology. Wettability evaluation for new and old acid-etched implants is shown. The “new” surface represents the implant immediately after acid-etching, while the “aged” surface represents a 4-week-old implant after acid-etching (stored for 4 weeks in a dark condition). Both surfaces had identical surface topography as shown in Fig. 3A. Representative images show a 3 μ L water droplet placed on the surfaces with a histogram of measured contact angles. Data are presented as mean \pm standard deviation ($n = 3$). *** $P < 0.001$. **** $P < 0.0001$.

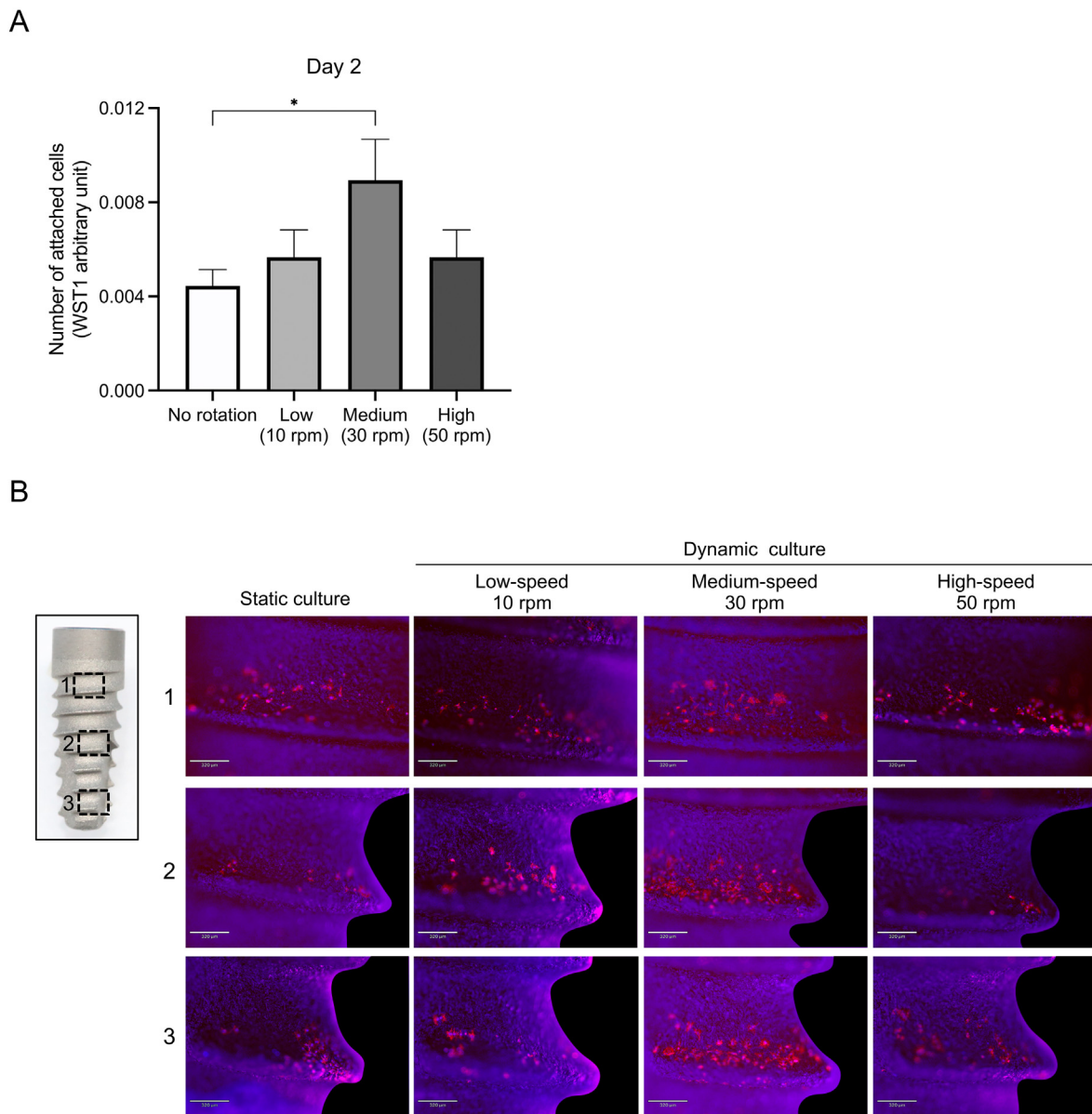


Figure 4 Osteoblast attachment efficiency in three-dimensional dynamic culture under different rotational speeds. (A) Quantification of osteoblasts attached to implant surfaces under various rotational conditions, assessed by the tetrazolium salt-based colorimetric assay (WST-1) on day 2 of culture. Data are presented as mean \pm standard deviation ($n = 3$). * $P < 0.05$. (B) Fluorescence microscopy images showing the distribution of osteoblasts across three different zones of the implant surfaces after day 2 under varied rotational speeds. Cells are dual-stained, with Rhodamine-phalloidin (red) for actin filaments and 4',6-diamidino-2-phenylindole (DAPI) (blue) for nuclei. Scale bar: 320 μm .

Discussion

The aim of this study was to develop and validate a novel 3D dynamic osteoblastic culture system for assessing the biological capabilities of dental implants in a clinically relevant manner. Utilizing real-life dental implants *in vitro*, our model bridges the gap between *in vitro* and *in vivo* experiments in implant research while retaining the advantages of traditional *in vitro* culture studies.

Validating the present 3D dynamic culture model is essential to ensure its reliability and relevance in replicating complex *in vivo* conditions. Our findings shed light

on several critical aspects of method validation, encompassing content, construct, and criterion validities.^{39,40}

Content validity assesses whether the study variables capture the necessary phenomena to address the research question. Static culture conditions led to uneven osteoblast attachment on standing dental implants due solely to gravity's influence on cell migration, making adherence to undercut areas challenging. To overcome this, we implemented dynamic flow of culture medium to promote constant cell circulation and exposure to the entire implant surface. Our optimized rotation speed of 30 rpm resulted in uniform attachment and proliferation of osteoblasts from

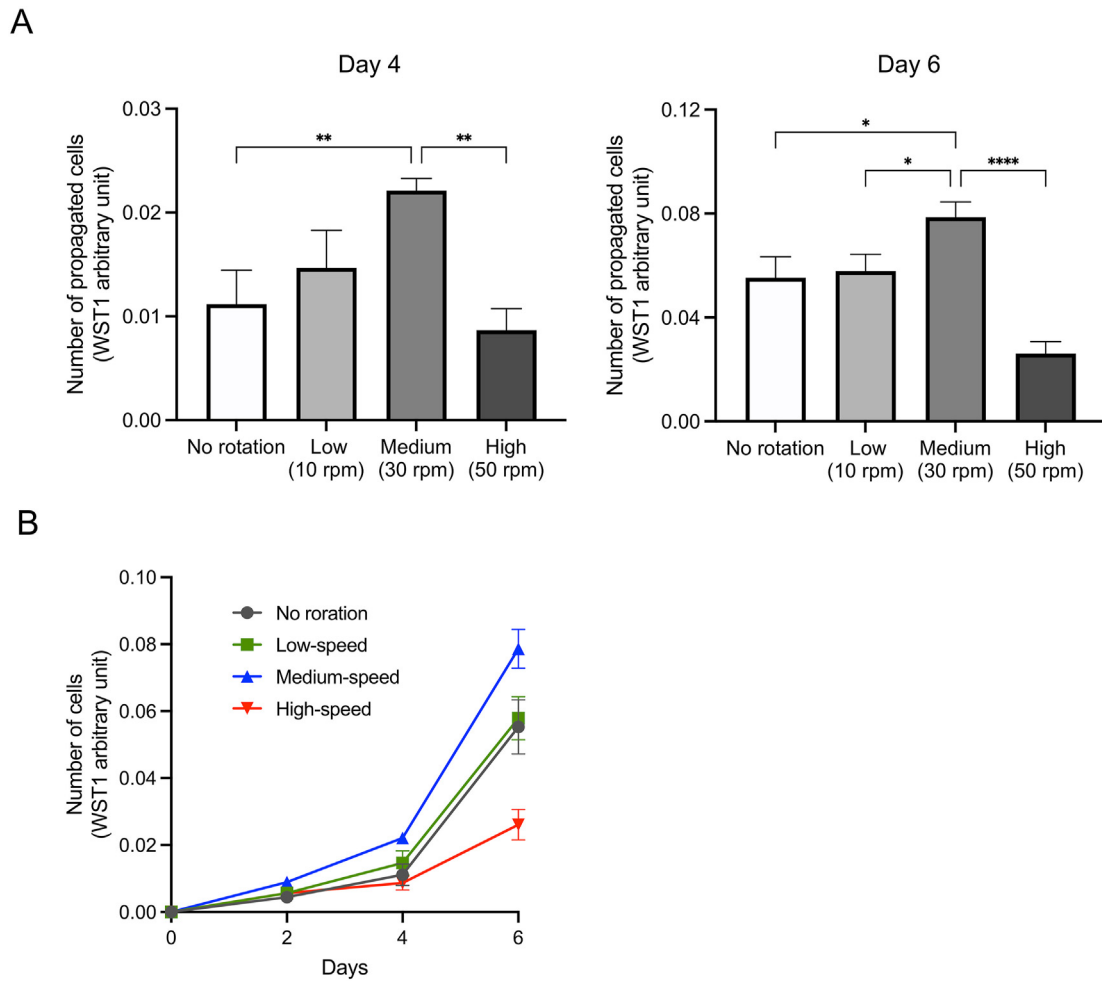


Figure 5 Osteoblast proliferation in response different rotational speeds. (A) The number of propagated osteoblasts on implant surfaces on days 4 and 6 under different rotational speeds. Data are presented as mean \pm standard deviation ($n = 3$). $*P < 0.05$. $**P < 0.01$. $****P < 0.0001$. (B) Growth curve illustrating osteoblast proliferation over time, measured at days 2, 4, and 6 of culture.

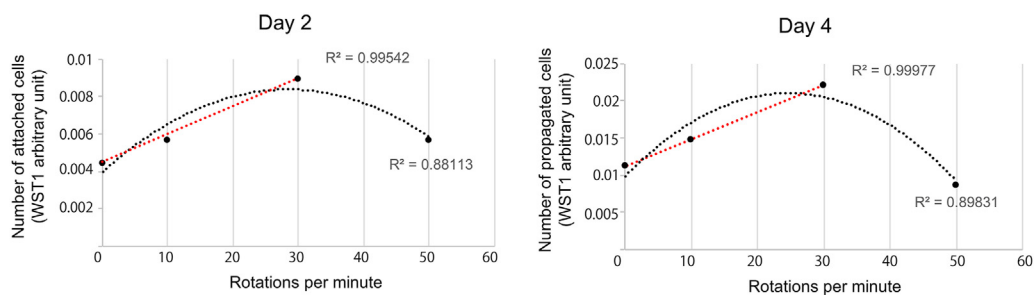


Figure 6 Influence of rotation speed on osteoblast attachment in three-dimensional dynamic culture. The graph illustrates the relationship between rotation speed and the number of osteoblasts attached to implant surfaces, plotted separately for days 2 and 4 of culture. Regression analysis revealed a linear correlation when data at 50 rpm were excluded, and a quadric curve when all data points were considered.

apex to coronal region. The significant correlation between rotation speed and attached cells validates this approach. Additionally, identifying the optimal speed (30 rpm) enhances content validity by showing that controlled rotation facilitates cell circulation without settling. Excessively fast circulation reduced cell attachment, aligning with previous

computer fluid dynamics studies, which revealed protein attachment is maximized with slow peri-implant blood flow.^{30,31} Thus, the optimal fluid flow rate is one that is fast enough to prevent cells from settling on the polystyrene dish and slow enough to allow them to settle on implant surfaces—30 rpm in our model.

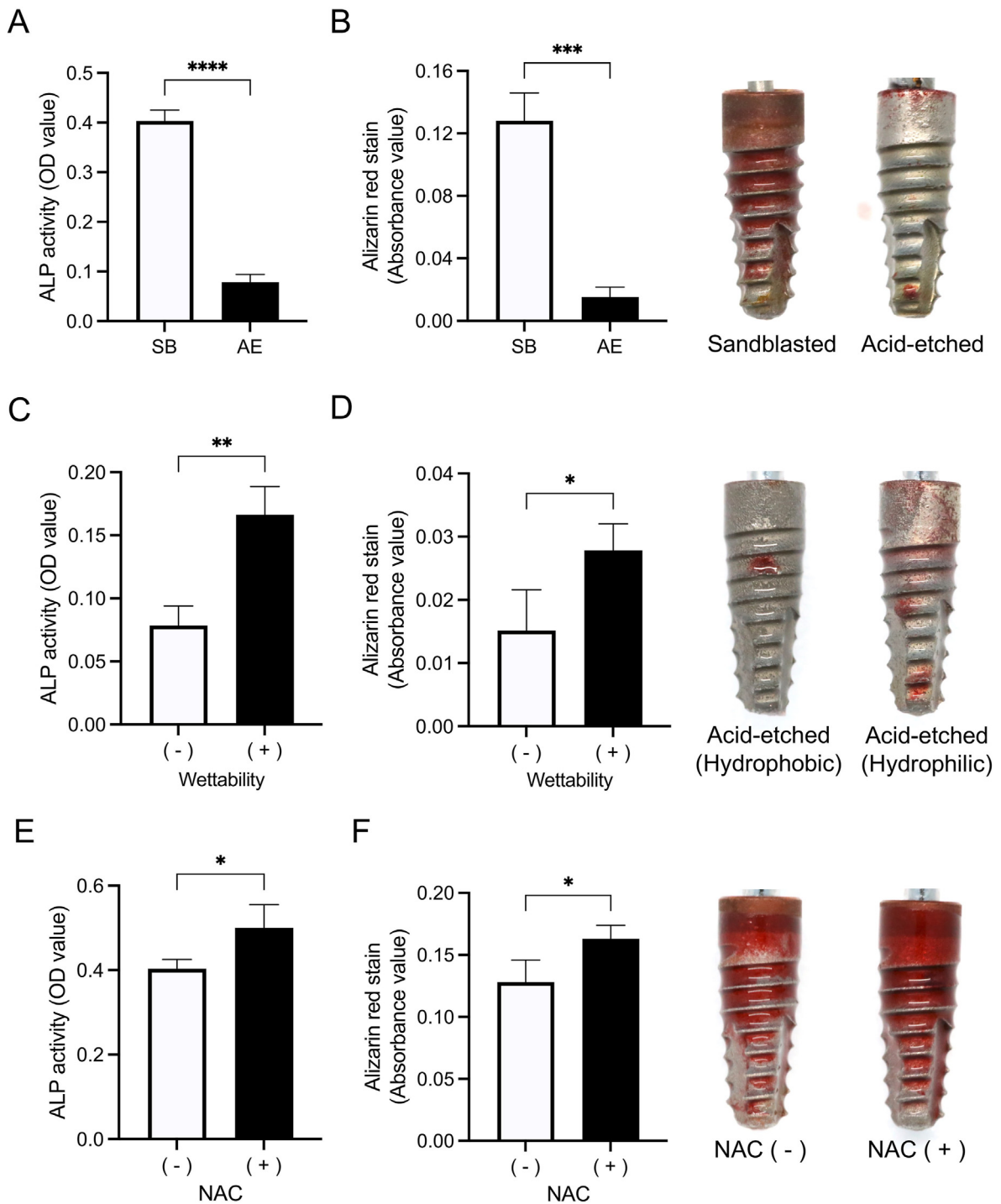


Figure 7 Influence of surface and environmental factors on osteogenic response. (A) Comparison of day 5 alkaline phosphatase (ALP) activity between sandblasted versus acid-etched implants. (B) Assessment of matrix mineralization by alizarin red staining on day 10 and representative images of sandblasted and acid-etched implants. (C) Comparison of ALP activity between hydrophobic versus hydrophilic implants. (D) Assessment of matrix mineralization and representative images of implants for both hydrophobic and hydrophilic surface. (E) Changes in ALP activity with or without N-acetylcysteine (NAC) supplementation to the culture medium. (F) Assessment of matrix mineralization and representative images of stained implants with and without NAC supplementation. Data are presented as mean \pm standard deviation ($n = 3$). * $P < 0.05$. ** $P < 0.01$. *** $P < 0.001$. **** $P < 0.0001$.

Construct validity ensures that the selected variables align with established concepts. We assessed the construct validity of our culture method by evaluating cellular

responses to implant surface topography, surface wettability, and biochemical supplements. Our dynamic culture model showed that implants with higher roughness had

higher ALP activity and mineralization compared to implants with lower roughness, establishing construct validity. The significant enhancement in osteoblast differentiation on hydrophilic microrough surfaces further supports this. Additionally, we tested the responsiveness of this dynamic culture to exogenous biochemical stimulation. Previous studies showed that NAC supplementation mitigates oxidative stress, enhancing cellular phenotypes.^{41–44} Although our study did not apply oxidative stress aggressively, it is present in the culture, particularly affecting osteoblasts due to microrough texture. NAC may have alleviated this stress. Our culture model confirmed up-regulated differentiation markers with NAC, validating the sensitivity of our dynamic culture model and supporting its construct validity. This high-sensitivity 3D culture system has the potential to be a valuable tool for studying the cellular impacts and underlying mechanisms of NAC as well as other supplements.

Criterion validity evaluates if a new method measures a concept in a manner consistent with existing methods. Our dynamic culture with 30 rpm exhibited an exponential increase in the number of cells present on implant surfaces with increasing culture time. Not only did the initial attachment of cells increase, but the retention of cells without dislodgement, even under dynamic conditions, likely contributed to this outcome. Considering the typical doubling time of osteoblasts, the rate of cell number increase found in our study aligns with the common understanding and results reported in the literature using similar rat bone marrow-derived osteoblasts.¹⁹ The ALP and alizarin red staining results measured in our culture model also aligns with common documentation of osteoblast behavior *in vitro*, further supporting criterion validity. Although we did not assess transcriptional profiles of osteoblasts, the observed ALP activity and mineralization, which appropriately responded to the culture environment and implant surface characteristics, suggest that changes in the expression of underlying osteogenic genes preceded these observations. Future studies should include mRNA profiling to complement the current findings and provide a more robust validation of the proposed 3D osteoblast culture method at the molecular biology level. Additionally, it is important to note that this study used rat-derived osteoblasts to validate the new culture system. Rat-derived osteoblasts differ from human osteoblasts in terms of cell proliferation capacity and mineralization efficiency,²⁶ which may lead to variations in responses to surface topographies and biochemical signals. However, an *in vitro* study testing novel implant surfaces with both rat-derived and human osteoblasts showed no significant differences in differentiation responses between cell types.⁴⁵ Therefore, while preliminary validation of culture duration might be prudent when applying different cell types in our 3D culture method, existing evidence suggests similar differentiation responses.

The developed 3D dynamic culture system represents a significant advancement in implant research, providing a more clinically and physiologically relevant platform for evaluating implant surfaces and studying osseointegration. Future studies could explore new factors potentially influencing osteoblast behavior and function, such as novel surface topographies, incorporation of growth factors and

biomolecules, or simulation of various host systemic conditions in the culture system.

In conclusion, this study highlights the need for more clinically relevant *in vitro* models in implant research and developed a novel 3D dynamic osteoblastic culture for dental implants. Our model allows evaluation of osteoblast attachment and function on dental implants *in vitro* and replicates optimized liquid flow around implants. Rigorous validation showed the system's sensitivity in discerning osteoblastic activity differences due to implant surface characteristics, and local biochemical factors. By offering a more physiologically relevant environment, this *in vitro* system has significant potential to advance implant research and development.

Declaration of competing interest

The authors have no conflicts of interest relevant to this article.

Acknowledgements

This study was supported by BioHorizons Implant Systems, Inc. Research Fund.

References

- Schneider GB, Perinpanayagam H, Clegg M, et al. Implant surface roughness affects osteoblast gene expression. *J Dent Res* 2003;82:372–6.
- Cooper LF, Masuda T, Yliheikkilä PK, Felton DA. Generalizations regarding the process and phenomenon of osseointegration. Part II. *In vitro* studies. *Int J Oral Maxillofac Implants* 1998;13:163–74.
- Wennerberg A, Albrektsson T. Suggested guidelines for the topographic evaluation of implant surfaces. *Int J Oral Maxillofac Implants* 2000;15:331–44.
- Wennerberg A, Albrektsson T. Effects of titanium surface topography on bone integration: a systematic review. *Clin Oral Implants Res* 2009;20(Suppl 4):172–84.
- Masaki C, Schneider GB, Zaharias R, Seabold D, Stanford C. Effects of implant surface microtopography on osteoblast gene expression. *Clin Oral Implants Res* 2005;16:650–6.
- Butz F, Ogawa T, Nishimura I. Interfacial shear strength of endosseous implants. *Int J Oral Maxillofac Implants* 2011;26:746–51.
- Ogawa T, Ozawa S, Shih JH, et al. Biomechanical evaluation of osseous implants having different surface topographies in rats. *J Dent Res* 2000;79:1857–63.
- Uno M, Hayashi M, Ozawa R, Saruta J, Ishigami H, Ogawa T. Mechanical interlocking capacity of titanium with respect to surface morphology and topographical parameters. *J Dent Oral Biol* 2020;5:1163.
- Ogawa T, Nishimura I. Different bone integration profiles of turned and acid-etched implants associated with modulated expression of extracellular matrix genes. *Int J Oral Maxillofac Implants* 2003;18:200–10.
- Ogawa T, Nishimura I. Genes differentially expressed in titanium implant healing. *J Dent Res* 2006;85:566–70.
- Ozawa S, Ogawa T, Iida K, et al. Ovariectomy hinders the early stage of bone-implant integration: histomorphometric, biomechanical, and molecular analyses. *Bone* 2002;30:137–43.

12. Saruta J, Sato N, Ishijima M, Okubo T, Hirota M, Ogawa T. Disproportionate effect of sub-micron topography on osteoconductive capability of titanium. *Int J Mol Sci* 2019;20:4027.
13. Komatsu K, Matsuura T, Suzumura T, Ogawa T. Genome-wide transcriptional responses of osteoblasts to different titanium surface topographies. *Mater Today Bio* 2023;23:100852.
14. Kubo K, Tsukimura N, Iwasa F, et al. Cellular behavior on TiO₂ nanonodular structures in a micro-to-nanoscale hierarchy model. *Biomaterials* 2009;30:5319–29.
15. Yamada M, Ueno T, Minamikawa H, Ikeda T, Nakagawa K, Ogawa T. Early-stage osseointegration capability of a sub-microfeatured titanium surface created by microroughening and anodic oxidation. *Clin Oral Implants Res* 2013;24:991–1001.
16. Tsukimura N, Ueno T, Iwasa F, et al. Bone integration capability of alkali- and heat-treated nanobimorphic Ti-15Mo-5Zr-3Al. *Acta Biomater* 2011;7:4267–77.
17. Nakamura H, Shim J, Butz F, Aita H, Gupta V, Ogawa T. Glycosaminoglycan degradation reduces mineralized tissue-titanium interfacial strength. *J Biomed Mater Res* 2006;77:478–86.
18. Nakamura HK, Butz F, Saruwatari L, Ogawa T. A role for proteoglycans in mineralized tissue-titanium adhesion. *J Dent Res* 2007;86:147–52.
19. Takeuchi K, Saruwatari L, Nakamura HK, Yang JM, Ogawa T. Enhanced intrinsic biomechanical properties of osteoblastic mineralized tissue on roughened titanium surface. *J Biomed Mater Res* 2005;72A:296–305.
20. Tabuchi M, Hamajima K, Tanaka M, Sekiya T, Hirota M, Ogawa T. UV light-generated superhydrophilicity of a titanium surface enhances the transfer, diffusion and adsorption of osteogenic factors from a collagen sponge. *Int J Mol Sci* 2021;22:6811.
21. Lee JH, Ogawa T. The biological aging of titanium implants. *Implant Dent* 2012;21:415–21.
22. Liu L, Wu J, Lv S, et al. Synergistic effect of hierarchical topographic structure on 3D-printed Titanium scaffold for enhanced coupling of osteogenesis and angiogenesis. *Mater Today Bio* 2023;23:100866.
23. Vashishat A, Patel P, Das Gupta G, Das Kurmi B. Alternatives of animal models for biomedical research: a comprehensive review of modern approaches. *Stem Cell Rev Rep* 2024;20:881–99.
24. Sivoilella S, Brunello G, Ferroni L, et al. A novel in vitro technique for assessing dental implant osseointegration. *Tissue Eng C Methods* 2016;22:132–41.
25. Ehlicke F, Berndt J, Marichikj N, et al. Biomimetic in vitro test system for evaluation of dental implant materials. *Dent Mater* 2020;36:1059–70.
26. Taylor SE, Shah M, Orriss IR. Generation of rodent and human osteoblasts. *BoneKEy Rep* 2014;3:585.
27. Sladkova-Faure M, Pujari-Palmer M, Ohman-Magi C, et al. A biomimetic engineered bone platform for advanced testing of prosthetic implants. *Sci Rep* 2020;10:22154.
28. Kitajima H, Hirota M, Iwai T, et al. Computational fluid simulation of fibrinogen around dental implant surfaces. *Int J Mol Sci* 2020;21:660.
29. Kitajima H, Hirota M, Iwai T, Mitsudo K, Saruta J, Ogawa T. Synergistic enhancement of protein recruitment and retention via implant surface microtopography and superhydrophilicity in a computational fluid dynamics model. *Int J Mol Sci* 2023;24:15618.
30. Kitajima H, Hirota M, Osawa K, et al. The effects of a biomimetic hybrid meso- and nano-scale surface topography on blood and protein recruitment in a computational fluid dynamics implant model. *Biomimetics* 2023;8:376.
31. Kitajima H, Hirota M, Osawa K, et al. Optimization of blood and protein flow around superhydrophilic implant surfaces by promoting contact hemodynamics. *J Prosthodont Res* 2022;67:568–82.
32. Park G, Matsuura T, Komatsu K, Ogawa T. Optimizing implant osseointegration, soft tissue responses, and bacterial inhibition: a comprehensive narrative review on the multifaceted approach of the UV photofunctionalization of titanium. *J Prosthodont Res* (online ahead of print).
33. Komatsu K, Hamajima K, Ozawa R, Kitajima H, Matsuura T, Ogawa T. Novel tuning of PMMA orthopedic bone cement using TBB initiator: effect of bone cement extracts on bioactivity of osteoblasts and osteoclasts. *Cells* 2022;11:3999.
34. Yamada M, Tsukimura N, Ikeda T, et al. N-acetyl cysteine as an osteogenesis-enhancing molecule for bone regeneration. *Biomaterials* 2013;34:6147–56.
35. Chao D, Komatsu K, Matsuura T, et al. Human gingival fibroblast growth and function in response to laser-induced meso- and microscale hybrid topography on dental implant healing abutments. *Int J Oral Maxillofac Implants* (online ahead of print).
36. Komatsu K, Matsuura T, Ogawa T. Achieving complete human gingival fibroblast collagen coverage on implant abutments through vacuum ultraviolet (VUV) photofunctionalization. *Int J Oral Maxillofac Implants* 2024;0:1–32.
37. Orriss IR, Hajjawi MO, Huesa C, MacRae VE, Arnett TR. Optimisation of the differing conditions required for bone formation in vitro by primary osteoblasts from mice and rats. *Int J Mol Med* 2014;34:1201–8.
38. Liu B, Lu Y, Wang Y, Ge L, Zhai N, Han J. A protocol for isolation and identification and comparative characterization of primary osteoblasts from mouse and rat calvaria. *Cell Tissue Bank* 2019;20:173–82.
39. Ogawa T, Tanaka M, Ogimoto T, Okushi N, Koyano K, Takeuchi K. Mapping, profiling and clustering of pressure pain threshold (PPT) in edentulous oral mucosa. *J Dent* 2004;32:219–28.
40. Ogawa T, Ogimoto T, Koyano K. Validity of the examination method of occlusal contact pattern relating to mandibular position. *J Dent* 2000;28:23–9.
41. Att W, Yamada M, Kojima N, Ogawa T. N-Acetyl cysteine prevents suppression of oral fibroblast function on poly(methylmethacrylate) resin. *Acta Biomater* 2009;5:391–8.
42. Yamada M, Kojima N, Paranjpe A, et al. N-acetyl cysteine (NAC)-assisted detoxification of PMMA resin. *J Dent Res* 2008;87:372–7.
43. Matsuura T, Komatsu K, Ogawa T. N-acetyl cysteine-mediated improvements in dental restorative material biocompatibility. *Int J Mol Sci* 2022;23:15869.
44. Xi X, Li ZX, Zhao Y, Liu H, Chen S, Liu DX. N-acetylcysteine promotes cyclic mechanical stress-induced osteogenic differentiation of periodontal ligament stem cells by downregulating Nrf2 expression. *J Dent Sci* 2022;17:750–62.
45. Kitajima H, Komatsu K, Matsuura T, et al. Impact of nano-scale trabecula size on osteoblastic behavior and function in a meso-nano hybrid rough biomimetic zirconia model. *J Prosthodont Res* 2023;67:288–99.